Diffusive diffraction measured with MRI at 7T

E. Gedat[1], S. Müller[2], T. Tolxdorff[1], J. Braun[1]

[1]Charité Universitätsmedizin Berlin, Institut für Medizinische Informatik, Berlin, Germany, [2]Charité Universitätsmedizin Berlin, Klinik für Neurologie, Berlin, Germany

Problem: Diffusion Weighted Imaging provides contrast with respect to the trace of the diffusion tensor. Diffusion Tensor Imaging (DTI) focuses on the direction of the highest eigenvalue. Diffusive diffraction patterns may be useful for probing the slow diffusion direction in tissues with geometrically uniform hydrophobic boundaries, for example the cylindrically shaped axonal myelin sheaths. Diffusive diffraction was predicted by Callaghan [1] and observed for water in a single capillary in an NMR experiment by Gibbs [2]. In this research a model system consisting in a bundle of water-filled capillaries with 100 µm inner diameter was studied to show principle observability of diffusive diffraction with MRI.

Materials and Methods: A bundle of 55 water-filled glass-capillaries with inner diameter of $2R$=100µm and length $L\cong$4cm was placed in a quadrupolar volume coil in a 7T Bruker BioSpec tomograph. Diffusion measurements were performed using a volume selective STEAM sequence with TE=20ms, δ=2.6ms, Δ=1000ms, TR=3000ms and a voxel of 10×10×50 mm^3 that contained the whole sample. For both directions of the diffusion gradients, parallel (Z) and perpendicular (Y) to the capillaries' axes, 32 points with arithmetically spaced gradient strength 0mT/m≤G≤230mT/m were recorded at a target temperature in the gradient bore of T=17.9°C. The echoes were Fourier-transformed and integrated in the frequency domain. The echo attenuation curves $A(q)$ were fitted with respect to the inner radius of the capillaries R and the diffusion coefficient D using the equation given by Söderman and Jönsson [3] with summation over the angle φ of the individual capillary axis with respect to the magnetic field gradient:

$$A(q)=\sum_{\varphi} p(\varphi)\sum_{n=0}^{n_{max}}\sum_{k=1}^{k_{max}}\sum_{m=0}^{m_{max}}\frac{2K_{nm}R^2(2\pi qR)^4\sin^2(2\varphi)\times\left[1-(-1)^n\cos(2\pi qL\cos\varphi)\right]\alpha_{km}^2}{L^2\left[(n\pi R/L)-(2\pi R)^2\cos^2\varphi\right]^2\times\left[\alpha_{km}^2-(2\pi qR)^2\sin^2\varphi\right]^2\left(\alpha_{km}^2-m^2\right)}\times\left[J_m'(2\pi qR\sin\varphi)\right]^2\times\exp\left\{-\left[\left(\frac{\alpha_{km}}{R}\right)^2+\left(\frac{n\pi}{L}\right)^2\right]D\Delta\right\} \quad (1)$$

With $q\equiv\gamma G\delta/2\pi$, $p(\varphi)$ is the probability for angle φ. K_{nm}={1 or 2 or 4 depending on n and m}, J_m is the Bessel function of order m, D the diffusion coefficient, and α_{km} are the roots of the Bessel function. Summation limits were k_{max}=6, including the sixth root of the Bessel function, m_{max}=9 including the m-th order Bessel function, and n_{max}={250; 3000} for Y- and Z-direction, respectively. The orientations of the capillaries' axes were determined independently by image analysis.

Results: The normalized stimulated echo intensities of water in the capillaries for the two gradient orientations are displayed in Figure 1. Clearly visible are the two diffraction minima at 0.66 and 1.13 qR in Y-direction. The fit of Eq. (1) yielded an inner diameter of the capillaries of $2R$=110µm. These minima are not present in Z-direction. The fit of Eq. (1) with respect to the diffusion coefficient yielded D=1.98×10^{-9}m^2/s for Y-direction and D=2.06×10^{-9}m^2/s for Z-direction. In Z-direction the data can also be simulated well with ordinary diffusion and D=2.05×10^{-9}m^2/s. Also visible is the higher echo amplitude for all points in Y-direction, which accounts for a smaller diffusion eigenvalue in the ordinary diffusion approximation of DTI at low qR. The angles in increments of 1° were φ={85;86;87;88;89;90}° with $p(\varphi)$={1;2;12;13;21;6}/55 in Y-direction and φ={0;1;2;3;4;5}° with $p(\varphi)$={0;9;15;16;11;4}/55 in Z-direction.

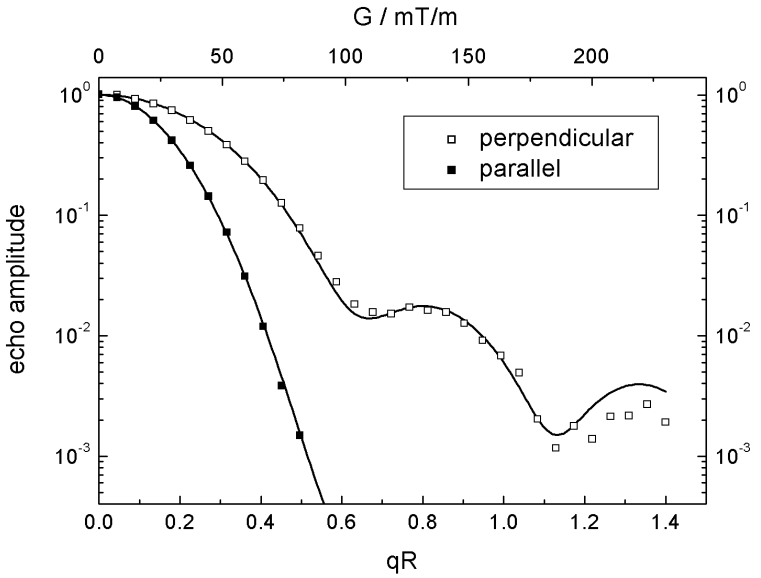

Figure 1: Normalized echo amplitudes of the diffusion measurements (symbols) and fitted theoretical curves according to Eq. (1) (lines).

Conclusion: The observation of diffusive diffraction with an MR-tomograph and a volume selective sequence is possible. The method may be applied to ordered biological systems like the spinal cord or muscle fibre.

References:

[1] Callaghan PT, *Principles of Nuclear Magnetic Resonance Microscopy*, Clarendon Press, Oxford 1991, pp. 371 ff.

[2] Gibbs SJ, *Observation of Diffusive Diffraction in a Cylindrical Pore by PFG NMR*, J Magn Reson 124, 223-226 (1997).

[3] Söderman O, Jönsson B, *Restricted Diffusion in Cylindrical Geometry*, J Magn Reson A 117, 94-97 (1995).